

# Spectra and total energies from self-consistent many-body perturbation theory

Arno Schindlmayr\* and Thomas J. Pollehn†

Cavendish Laboratory, University of Cambridge, Madingley Road, Cambridge CB3 0HE, United Kingdom

R. W. Godby

Department of Physics, University of York, Heslington, York YO10 5DD, United Kingdom

(Received 9 June 1998)

With the aim of identifying universal trends, we compare fully self-consistent electronic spectra and total energies obtained from the  $GW$  approximation with those from an extended  $GWT$  scheme that includes a nontrivial vertex function and the fundamentally distinct Bethe–Goldstone approach based on the  $T$ -matrix. The self-consistent Green’s function  $G$ , as derived from Dyson’s equation, is used not only in the self-energy but also to construct the screened interaction  $W$  for a model system. For all approximations we observe a similar deterioration of the spectrum, which is not removed by vertex corrections. In particular, satellite peaks are systematically broadened and move closer to the chemical potential. The corresponding total energies are universally raised, independent of the system parameters. Our results therefore suggest that any improvement in total energy due to self-consistency, such as for the electron gas in the  $GW$  approximation, may be fortuitous.

PACS numbers: 71.10.-w, 71.45.Gm, 71.15.Nc

## I. INTRODUCTION

Thanks to advances in modern computer technology and an increasingly efficient treatment of the underlying one-electron structure, many-body corrections to the quasiparticle band energies and spectral functions of solids can now be obtained from first principles using many-body perturbation theory. Most calculations for real materials employ the  $GW$  approximation,<sup>1</sup> which owes its name to the fact that it models the electron self-energy as the product  $\Sigma^{GW} = iGW$  of the Green’s function  $G$  and the dynamically screened Coulomb interaction  $W$ . By explicitly including polarization effects in the exchange term it describes dynamic correlation between the electrons and so can be physically motivated as an extension of the static Hartree–Fock treatment.

The Green’s function of the interacting electron system is linked to the self-energy by means of Dyson’s equation, symbolically written as  $G^{-1} = G^{\text{H}}^{-1} - \Sigma$ , where  $G^{\text{H}}$  indicates the Hartree approximation that neglects both exchange and correlation. It is immediately clear that one faces a self-consistency problem, because the self-energy in turn depends on the Green’s function. Hence both propagators must be determined simultaneously. The latter functional dependence is of course nonlinear due to the dynamic properties of the screened interaction, which is related to the bare Coulomb potential  $v$  and the polarizability  $P$  through  $W^{-1} = v^{-1} - P$ . In a manner consistent with the  $GW$  approximation the neglect of vertex corrections in the polarizability yields the random-phase approximation  $P^{\text{RPA}} = -2iGG$ , which ignores the interaction between the screening electrons and holes.

To obtain full self-consistency the above four equations have to be solved iteratively starting from a zeroth-order noninteracting Green’s function until the results stabilize. Although self-consistent  $GW$  calculations for real materials are now within reach,<sup>2</sup> the associated compu-

tational cost is still enormous. Therefore in practice the outcome of the first iteration is instead taken as the final spectrum. In this formulation the  $GW$  approximation has been applied to a wide range of materials including semiconductors<sup>3–5</sup> and alkali metals<sup>6</sup> as well as transition metals<sup>7</sup> and their oxides.<sup>8</sup> For all these diverse systems the predicted quasiparticle band structures agree very well with experimental results, while optical spectra, which include satellite features resulting from collective excitations such as plasmons, are generally less satisfactory and require the addition of so-called vertex corrections. However, systematic progress in this direction is still limited.<sup>9</sup>

Despite the apparent success of conventional calculations, the neglect of self-consistency remains problematic, in part because it implies a certain ambiguity with respect to the choice of starting point. The zeroth-order Green’s function is usually constructed from the local-density approximation (LDA), but in principle it is equally possible to start from any other initial approximation such as the Hartree–Fock treatment.<sup>5</sup> The resulting spectra will in general differ.<sup>10</sup> Furthermore, the non-self-consistent  $GW$  scheme violates the Baym–Kadanoff criteria for conserving approximations.<sup>11</sup> As a result the total particle number, energy, and momentum of the system are not conserved under the influence of external perturbations. Even without such perturbations, the integrated spectral weight no longer corresponds to the number of physical particles.<sup>12</sup>

In order to address these issues, past implementations have occasionally incorporated modifications aimed at introducing a higher degree of self-consistency. In particular, the band energies of the zeroth-order Green’s function used to evaluate the self-energy are sometimes shifted such as to improve agreement with those obtained from Dyson’s equation.<sup>3,6,8</sup> This approach assumes that the true quasiparticle orbitals are virtually indistinguish-

able from the corresponding LDA wave functions, which has only been explicitly proven for states close to the band edge of simple semiconductors, however.<sup>3</sup> Moreover, it entirely ignores the transfer of spectral weight to satellite peaks, which typically account for between 10% and 50% of the total spectrum.

More properly self-consistent results for model systems were recently reported, although most realizations still restrict the computational expense by fixing the screening function  $W$  either at the zeroth-order random-phase approximation<sup>13–15</sup> or a simpler plasmon-pole model.<sup>16</sup> Until now the only comprehensive, fully self-consistent calculations have been performed for a quasi-one-dimensional semiconducting wire<sup>17,18</sup> and the homogeneous electron gas.<sup>19,20</sup> For the electron gas, the system most studied so far,<sup>14–16,19,20</sup> self-consistency was found to *worsen* the agreement between calculated spectra and exact results by (i) increasing the occupied bandwidth, (ii) transferring weight from the plasmon satellites to the corresponding quasiparticle peaks, (iii) narrowing the quasiparticle resonance widths, thereby increasing the lifetime, and (iv) broadening the plasmon satellites while moving them closer to the Fermi surface. Some of these effects have also been observed for the quasi-one-dimensional wire,<sup>18</sup> and there is evidence that the reported increase in the band gap extends to real semiconductors.<sup>2</sup> In contrast, self-consistency *improves* the agreement of quasiparticle energies of localized semi-core states with experimental data.<sup>13</sup>

Because of the small number of models studied so far the results quoted above cannot readily be assumed for other systems without further quantitative investigations, nor is it clear whether they are peculiar to the  $GW$  approximation or of a more general nature. Previous partially self-consistent calculations that include vertex corrections have done little to clarify the situation, since they only consider modifications of the  $GW$  scheme in the form of additional self-energy diagrams of second order in  $W$ : depending on the choice of diagrams and the model screening function used, these may restore the occupied band width of the electron gas to its superior non-self-consistent value<sup>16</sup> or leave it unchanged.<sup>15</sup>

In order to shed more light on these numerical aspects, in this paper we present fully self-consistent calculations for a model system using a wide range of conserving self-energy approximations. Besides the  $GW$  approximation and an extended  $GWT$  scheme that is derived from time-dependent Hartree–Fock rather than Hartree theory and includes multiple particle–hole scattering,<sup>21</sup> we also consider the fundamentally distinct Bethe–Goldstone approach<sup>22</sup> based on the  $T$ -matrix. Our first objective is to compare the resulting spectra and thereby identify universal trends.

In the second part of this paper we then focus on total energies. A very interesting outcome of recent fully self-consistent calculations for the electron gas was that the total energy derived from the Green’s function is strikingly close to values obtained from quantum Monte-

Carlo simulations,<sup>19</sup> which are presumed accurate. It has been speculated that this unexpected result is related to the fact that the self-consistent  $GW$  scheme conserves energy,<sup>23</sup> but the basis of this connection is not immediately obvious. Rather, we will show here that self-consistency in fact systematically raises the total energy. Our results therefore suggest that the improvement for the electron gas may be fortuitous.

This paper is organized as follows. In Sec. II we present the model system and its exact numerical solution. In Sec. III we discuss the self-energy approximations considered here in more detail. In Secs. IV and V we give results for spectral functions and total energies, respectively. Finally, in Sec. VI we summarize our conclusions.

## II. MODEL DESCRIPTION

In order to limit the computational cost of fully self-consistent calculations with vertex corrections beyond the  $GW$  approximation, which so far have never been attempted for real materials, we consider a Hubbard model that describes the dynamics of electrons on a lattice with strong, short-range interaction. The Hamiltonian is sufficiently simple that it can be diagonalized exactly for small cluster sizes using standard numerical techniques, yet its physical behavior is nontrivial and reflects many properties of real materials. The model geometry we employ is a finite two-leg ladder with open boundary conditions. Each of the  $M$  lattice sites contains one orbital that can accommodate up to two electrons with opposite spin. Doubly occupied orbitals are penalized by a repulsive on-site interaction  $U$ , while the hopping of transient electrons between neighboring sites yields an energy gain of  $-t$ . The full Hamiltonian is

$$\mathcal{H} = -t \sum_{\langle \mathbf{R}, \mathbf{R}' \rangle, \sigma} c_{\mathbf{R}\sigma}^\dagger c_{\mathbf{R}'\sigma} + U \sum_{\mathbf{R}} \hat{n}_{\mathbf{R}\uparrow} \hat{n}_{\mathbf{R}\downarrow}, \quad (1)$$

where  $c_{\mathbf{R}\sigma}^\dagger$ ,  $c_{\mathbf{R}\sigma}$  are the creation and annihilation operators for an electron at site  $\mathbf{R}$  with spin  $\sigma$ ,  $\hat{n}_{\mathbf{R}\sigma} \equiv c_{\mathbf{R}\sigma}^\dagger c_{\mathbf{R}\sigma}$  is the particle number operator, and  $\langle \mathbf{R}, \mathbf{R}' \rangle$  indicates a sum over nearest neighbors only. We choose the energy norm by setting  $t = 1$ . The total electron number is denoted by  $N$ .

The exact one-particle Green’s function at zero temperature is defined as

$$G_{\mathbf{R}\mathbf{R}'}(t - t') = -i \langle N | \mathcal{T} \{ c_{\mathbf{R}\sigma}(t) c_{\mathbf{R}'\sigma}^\dagger(t') \} | N \rangle, \quad (2)$$

where  $|N\rangle$  is the ground state of the interacting many-electron system,  $\mathcal{T}$  is Wick’s time-ordering operator, and  $c_{\mathbf{R}\sigma}(t) \equiv \exp(i\mathcal{H}t) c_{\mathbf{R}\sigma} \exp(-i\mathcal{H}t)$  denotes the time-dependent wave-field operator in the Heisenberg picture. We have suppressed the spin index in  $G$  because the Green’s function is diagonal and degenerate in  $\sigma$ .

The Green’s function can in principle be written in terms of the eigenstates featuring an additional electron

or hole,<sup>24</sup> but this representation is disadvantageous because the basis set grows exponentially with the system size. While the Hamiltonian matrix contains mostly zeroes and so may be stored in a compressed format, the same is not possible for the eigenvector matrix since it is not in general sparse. For a reasonable system size the memory requirements thus render this procedure infeasible. Instead, we Fourier transform (2) to the energy domain and rewrite the Green's function in the form

$$G_{\mathbf{R}\mathbf{R}'}(\omega) = \langle N | c_{\mathbf{R}\sigma} \frac{1}{\omega - \mathcal{H}^+ + E_N + i\delta} c_{\mathbf{R}'\sigma}^\dagger | N \rangle + \langle N | c_{\mathbf{R}'\sigma}^\dagger \frac{1}{\omega + \mathcal{H}^- - E_N - i\delta} c_{\mathbf{R}\sigma} | N \rangle. \quad (3)$$

Here  $E_N$  is the ground-state energy corresponding to  $|N\rangle$ , which we compute by simultaneous subspace iteration,<sup>25</sup> and  $\mathcal{H}^\pm$  denotes the Hamiltonian matrix for  $N \pm 1$  electrons. The parameter  $\delta$  is positive and tends to zero. In practice we use a finite but small value of  $\delta = 0.05$ . The diagonal elements of  $G$ , in which we are most interested, may now be calculated without full matrix inversion by transforming  $\omega \mp (\mathcal{H}^\pm - E_N - i\delta)$  to a chain using the recursion method<sup>26</sup> and starting with the vector  $c_{\mathbf{R}'\sigma}^\dagger |N\rangle$  or  $c_{\mathbf{R}\sigma} |N\rangle$ . Once the diagonal elements  $a_n$  and off-diagonal elements  $b_n$  of the tridiagonal matrix are determined up to a suitable chain length  $D$ , the elements of the Green's function are obtained from

$$G_{\mathbf{R}\mathbf{R}}(\omega) = \frac{1}{\omega - a_0 - \frac{b_1^2}{\omega - a_1 - \dots - \frac{b_D^2}{\omega - a_D}}}. \quad (4)$$

For nondiagonal elements of  $G$  an analogous block recursion must be performed. As the Hamiltonians considered here have many highly degenerate eigenvalues, the chain length  $D$  can be chosen substantially lower than the order of  $\mathcal{H}^\pm$ . In practice a few recursions per actual spectral feature are sufficient to achieve full convergence. To check the accuracy we have also calculated the total particle number for all systems discussed in the following by summing the diagonal elements of  $G$  and integrating the spectral weight below the chemical potential  $\mu$ . The numerical deviation from the exact values is of the order of 0.1%.

### III. SELF-ENERGY APPROXIMATIONS

In many-body perturbation theory the effect of the Coulomb force on the propagation of quasiparticles is rigorously described by an effective potential. Following established conventions we distinguish between the Hartree contribution

$$V_{\mathbf{R}\mathbf{R}'}^H = U(\langle \hat{n}_{\mathbf{R}\uparrow} \rangle + \langle \hat{n}_{\mathbf{R}\downarrow} \rangle) \delta_{\mathbf{R}\mathbf{R}'} \quad (5)$$

and the remaining exchange-correlation part, which we call the self-energy  $\Sigma$ . It is in general both nonlocal and

energy-dependent. Although the exact self-energy functional remains elusive, physically motivated approximations can be obtained by truncating its diagrammatic series expansion. In the following we describe the three distinct schemes considered in this paper.

The  $GW$  approximation renormalizes the nonlocal Fock potential by including dynamic screening in the exchange interaction, as shown diagrammatically in Fig. 1(a). The screening function is modeled in the random-phase approximation (RPA) and includes ring diagrams to all orders. In the spirit of the space-time method<sup>27</sup> we avoid costly convolutions by switching between the real time and energy domains as appropriate, using fast Fourier transforms with 32,768 sampling points over a range of 160 energy units. This procedure also guarantees a high degree of numerical accuracy, because we do not need to repeatedly fit the propagators to analytic functions. Given a Green's function  $G$  we hence compute the self-energy by solving the defining equations

$$P_{\mathbf{R}\mathbf{R}'}^{\text{RPA}}(t) = -2iG_{\mathbf{R}\mathbf{R}'}(t)G_{\mathbf{R}'\mathbf{R}}(-t), \quad (6)$$

$$W_{\mathbf{R}\mathbf{R}'}^{-1}(\omega) = \frac{1}{U} \delta_{\mathbf{R}\mathbf{R}'} - P_{\mathbf{R}\mathbf{R}'}^{\text{RPA}}(\omega), \quad (7)$$

$$\Sigma_{\mathbf{R}\mathbf{R}'}^{GW}(t) = iG_{\mathbf{R}\mathbf{R}'}(t)W_{\mathbf{R}\mathbf{R}'}(t). \quad (8)$$

The factor 2 in the polarization propagator is due to spin summation.

While the  $GW$  approximation accurately describes materials that are governed by the screening of free carriers, such as the homogeneous electron gas, vertex corrections are in general necessary for more complex systems. Such extensions are often referred to as  $GWT$  schemes. A particular approximation that we consider here includes a vertex function derived from time-dependent Hartree-

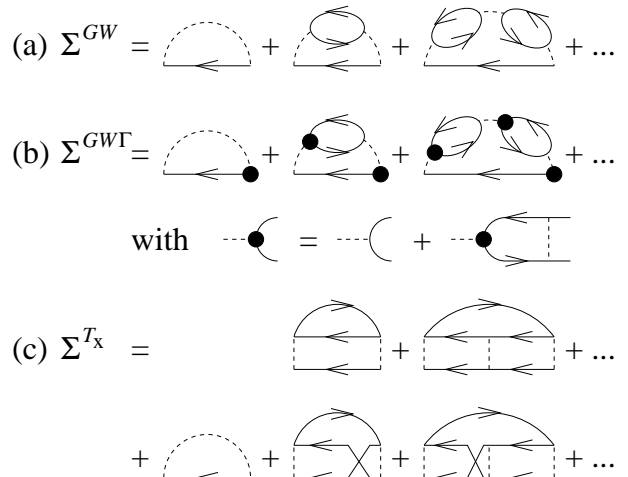


FIG. 1. Diagrammatic representation of (a) the  $GW$  approximation, (b) a  $GWT$  scheme with vertex corrections that describe multiple particle-hole scattering, and (c) the Bethe-Goldstone approach based on the  $T$ -matrix. Arrows represent Green's functions; the Coulomb interaction is indicated by a broken line.

Fock theory, as shown in Fig. 1(b). It contains multiple scattering in the particle–hole channel, which is most significant in atomic and molecular systems with partially filled shells.<sup>28</sup> Nontrivial vertex functions usually increase the computational cost dramatically, but due to the short-range interaction in the Hubbard model the self-energy in this case is still given by an expression of the form (8), albeit with a modified screened interaction

$$\tilde{W}_{\mathbf{R}\mathbf{R}'}^{-1}(\omega) = \frac{1}{U}\delta_{\mathbf{R}\mathbf{R}'} - \frac{1}{2}P_{\mathbf{R}\mathbf{R}'}^{\text{RPA}}(\omega). \quad (9)$$

The Bethe–Goldstone approach constitutes a fundamentally distinct approximation based on the so-called transition or  $T$ -matrix, which describes multiple scattering in the particle–particle and hole–hole channels to all orders. This process dominates in the low-density limit of the electron gas,<sup>29</sup> but it also predicts the specific behavior of systems with localized orbitals and strong electronic correlation such as the transition metals.<sup>30</sup> As the self-energy, shown as a sum of ladder diagrams in Fig. 1(c), contains exchange contributions in the two-particle propagator, we designate it by the label  $T_x$ . For the Hubbard model the corresponding direct and exchange terms are in fact identical except for a prefactor of 2 due to spin summation in the former, so the self-energy is given by

$$G_{\mathbf{R}\mathbf{R}'}^2(t) = iG_{\mathbf{R}\mathbf{R}'}(t)G_{\mathbf{R}\mathbf{R}'}(t), \quad (10)$$

$$T_{\mathbf{R}\mathbf{R}'}^{-1}(\omega) = \frac{1}{U}\delta_{\mathbf{R}\mathbf{R}'} - G_{\mathbf{R}\mathbf{R}'}^2(\omega), \quad (11)$$

$$\Sigma_{\mathbf{R}\mathbf{R}'}^{T_x}(t) = -iT_{\mathbf{R}\mathbf{R}'}(t)G_{\mathbf{R}'\mathbf{R}}(-t) - V_{\mathbf{R}\mathbf{R}'}^{\text{H}}\delta(t). \quad (12)$$

In the last equation we have subtracted the Hartree potential because it is already dealt with separately.

By tuning the parameters of the Hamiltonian (1) we can create configurations geared to the particular strengths of different self-energy approximations within the same model: independent of the Coulomb integral  $U$  the  $T$ -matrix becomes increasingly accurate for a very low or, because of particle–hole symmetry, very high fractional band filling  $N/(2M)$ , while the  $GW$  schemes perform best for medium site occupancies and a not too strong interaction.<sup>10</sup>

#### IV. SELF-CONSISTENT SPECTRA

In order to study the effects of self-consistency in a general perspective, we compare calculations using all the many-body approximations described in the previous section. As a convenient starting point we choose the Hartree Green's function  $G^{\text{H}}$ , which only includes the electrostatic potential  $V^{\text{H}}$  generated by the total electron charge. The occupation numbers  $\langle \hat{n}_{\mathbf{R}\sigma} \rangle$  are determined self-consistently by a simple iterative procedure. After evaluating the self-energy  $\Sigma$  we obtain an updated, dressed Green's function from Dyson's equation

$$G_{\mathbf{R}\mathbf{R}'}^{-1}(\omega) = G_{\mathbf{R}\mathbf{R}'}^{\text{H}-1}(\omega) - \Sigma_{\mathbf{R}\mathbf{R}'}(\omega), \quad (13)$$

which in a conventional treatment is taken as the final spectrum. In a self-consistent calculation we instead use it to compute a new Hartree potential and self-energy and continue the iteration until the results stabilize. To guarantee the correct analytic time-ordering of the spectrum obtained from Dyson's equation it is necessary to shift the Hartree Green's function rigidly on the energy axis by an amount  $\langle \Sigma(\mu^{\text{H}}) \rangle$  before evaluating the self-energy in (13). Here  $\mu^{\text{H}}$  denotes the chemical potential, which we identify with the highest occupied quasiparticle state, and the matrix element is formed with the corresponding orbital. As this shift must tend to zero for the self-consistent solution, we decrease it by a factor of  $e^{-1}$  in every subsequent iteration. To achieve convergence we typically perform at least ten iterations, after which the shift is reduced to a negligible value without influence on the spectral features or total energy. We use a very small initial resonance width of  $\delta = 0.05$  throughout the calculations in order to avoid systematic errors, and only the final spectra are broadened through convolution with a Lorentzian of width 0.5 for visual display. We have again checked the numerical reliability by calculating the total particle number from the self-consistent Green's functions and generally find the same high level of accuracy as for the exact solution.

In Fig. 2 we compare an ordinary  $GW$  spectral function, obtained from a single iteration of Dyson's equation, with the result of a converged, self-consistent calculation after 10 iterations. Like all other figures in this section it shows the diagonal element for a corner site of the cluster, which we have confirmed to be representative. The following observations therefore apply equally to other matrix elements. By setting the model parameters to  $M = 10$  and  $N = 2$  with a medium interaction strength

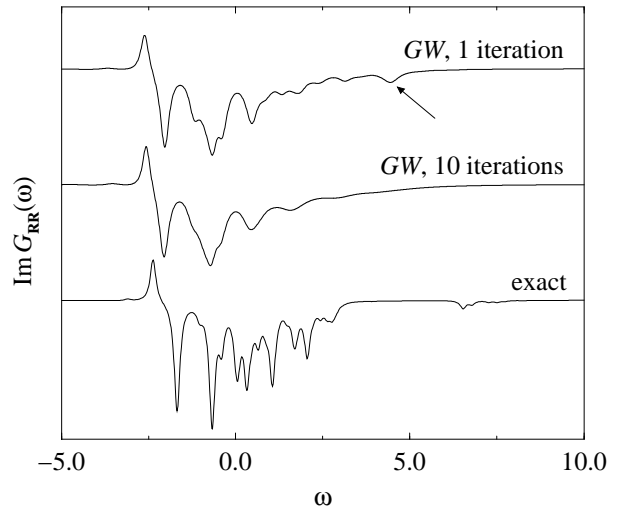


FIG. 2. Comparison between an ordinary and a converged  $GW$  calculation after 10 iterations. The most striking effect of self-consistency is the broadening of satellite peaks, which are hardly discernible in a diffuse background. This is particularly obvious at high energies, as indicated by an arrow.

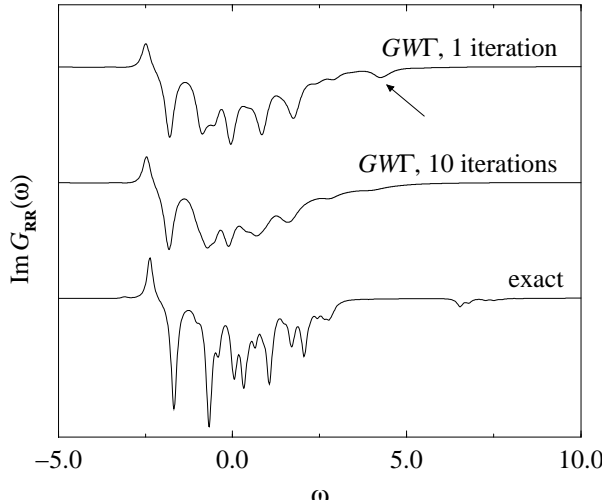


FIG. 3. The vertex function in the  $GWT$  approximation fails to prevent the deterioration of spectral features when brought to full self-consistency.

of  $U = 4$  we have deliberately chosen a small band filling of 10% for which the  $GW$  approximation is not optimal, so that possible improvements should be more obvious. The exact spectrum is shown for comparison.

To examine the effects of self-consistency we distinguish between quasiparticles and their satellites. The former are in fact little affected, mainly by small shifts in position and a marginal narrowing of the resonance width for states close to the chemical potential. In contrast, the satellite spectrum deteriorates significantly. The most striking change is the broadening of satellite peaks. By fitting the spectrum to a set of Lorentzians we find that the resonance widths approximately double. As the spectral weight is smeared out and peaks merge, individual features are hardly discernible above the spectral back-

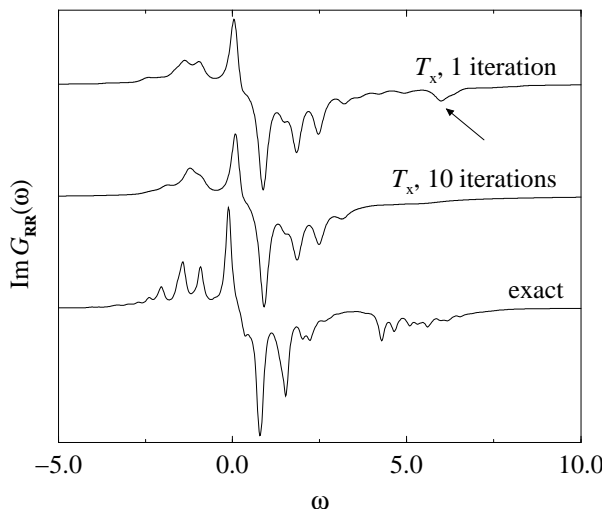


FIG. 4. Although unrelated to the  $GW$  approximation, the  $T_x$  scheme effects the same changes in quasiparticle and satellite peaks in a converged, self-consistent spectrum.

ground, particularly isolated satellites at high energies. One such example is indicated by an arrow. Furthermore, it can be seen that the satellites move closer towards the chemical potential. All of these observations are in agreement with previous self-consistent calculations.<sup>14,19</sup>

We now address the relation between self-consistency and the simultaneous inclusion of vertex corrections. To this end we show the results of a corresponding  $GWT$  calculation in Fig. 3. It is evident that the vertex function in the latter fails to prevent the deterioration of spectral features when brought to full self-consistency. In particular, we do not observe a restoration of well-defined structure. This point is further underlined by our investigation of the Bethe–Goldstone approach. A typical calculation using  $N = 6$ , which corresponds to a band filling of 30%, is illustrated in Fig. 4: although unrelated to the  $GW$  approximation, the  $T_x$  scheme effects the same changes in quasiparticle and satellite peaks in a converged, self-consistent spectrum.

The general success of ordinary  $GW$  calculations for most systems suggests that the sum of all neglected self-energy diagrams is small. A thorough understanding of this process is invaluable for the design of superior approximations, but despite continuing efforts the nature of this cancellation remains elusive. On the one hand, there is strong evidence for a certain mutual cancellation between corresponding vertex corrections in the polarizability and self-energy.<sup>31–33</sup> If we assume that this argument still holds for the true vertex function, then by extension the remaining contributions, i.e., the self-consistent renormalization of propagators in the polarizability and self-energy, must also cancel. However, the disturbing deterioration of spectral features in the self-consistent  $GW$  approximation,<sup>19</sup> particularly when compared to a partially self-consistent calculation with a fixed zeroth-order dielectric function,<sup>14</sup> suggests that this is not the case, at least when a trivial vertex is used. Consequently one would also expect a certain mutual cancellation between self-consistency and vertex diagrams. Recently reported direct numerical evidence<sup>16</sup> to this end is circumstantial, however, since only quasiparticle properties were considered and the response function was replaced by a plasmon-pole model of unclear diagrammatic structure. In this context our results, alongside those from a partially self-consistent cumulant expansion that also examined complete spectral functions,<sup>15</sup> indicate that this cancellation is a very subtle process and that mutually balancing contributions may be hard to identify.

## V. TOTAL ENERGIES

One of the notable features of self-consistency in many-body perturbation theory is that the total energy becomes a proper, uniquely defined quantity. In practice total energies are most often obtained from the one-particle Green's function using the Galitskii–Migdal formula,<sup>34</sup>

which may of course be applied to any approximate  $G$ . However, it is important to note that other definitions, for instance through the two-particle Green's function or an integral of the interaction strength, in general yield different numerical values. Full self-consistency removes this ambiguity. Moreover, the total energy is then also properly conserved under the influence of external perturbations.<sup>11</sup>

For the Hubbard model an analogous expression for the total energy

$$E = \frac{1}{\pi} \sum_{\langle \mathbf{R}, \mathbf{R}' \rangle} \int_{-\infty}^{\mu} (\omega \delta_{\mathbf{R}\mathbf{R}'} - t) \operatorname{Im} G_{\mathbf{R}\mathbf{R}'}(\omega) d\omega \quad (14)$$

in terms of the one-particle Green's function can be derived from the equation of motion of the wave-field operator. Despite formal similarities to the Galitskii–Migdal formula this expression also contains contributions from nondiagonal elements of the Green's function. The reason for this apparent discrepancy is that the site index  $\mathbf{R}$  does not represent a spatial coordinate. Instead, it is introduced in second quantization to label a set of overlapping Wannier orbitals. As the creation and annihilation operators are transformed separately, local operators in real space become nondiagonal in the site index, a point that was previously noted in conjunction with the proper parametrization of the charge density.<sup>35</sup> Analogously the local kinetic-energy operator and external potential correspond to the nondiagonal hopping term of the Hubbard Hamiltonian, which resurfaces here.

Unlike the calculation of the particle number, a direct evaluation of the frequency integral in (14) proved quite sensitive to the initial resonance width  $\delta$ . In order to obtain reliable results, we therefore fit the elements of the Green's function to a model of the form

$$G_{\mathbf{R}\mathbf{R}'}(\omega) = \sum_n \frac{a_{\mathbf{R}\mathbf{R}'}^n}{\omega - b_{\mathbf{R}\mathbf{R}'}^n - i\delta_{\mathbf{R}\mathbf{R}'}^n} + \sum_m \frac{a_{\mathbf{R}\mathbf{R}'}^m}{\omega - b_{\mathbf{R}\mathbf{R}'}^m + i\delta_{\mathbf{R}\mathbf{R}'}^m}, \quad (15)$$

which of course becomes exact as  $\delta$  tends to zero. The frequency integration can now be performed analytically in the proper limit  $\delta_{\mathbf{R}\mathbf{R}'}^n \rightarrow 0$ , and so for the total energy we eventually obtain

$$E = \sum_{\langle \mathbf{R}, \mathbf{R}' \rangle} \sum_n (b_{\mathbf{R}\mathbf{R}'}^n \delta_{\mathbf{R}\mathbf{R}'} - t) a_{\mathbf{R}\mathbf{R}'}^n. \quad (16)$$

We have confirmed the reliability of our procedure by comparing total energies derived from the true Green's function with the exact numerical value  $E_N$ , which we obtained earlier by diagonalizing the Hamiltonian matrix. The fit according to (15) is very accurate. Unfortunately it is also computationally expensive, so that all results in this section refer to a reduced model size of  $M = 6$ .

In Figs. 5 and 6 we show calculated total energies as a function of the interaction strength  $U$  for  $N = 2$ , which

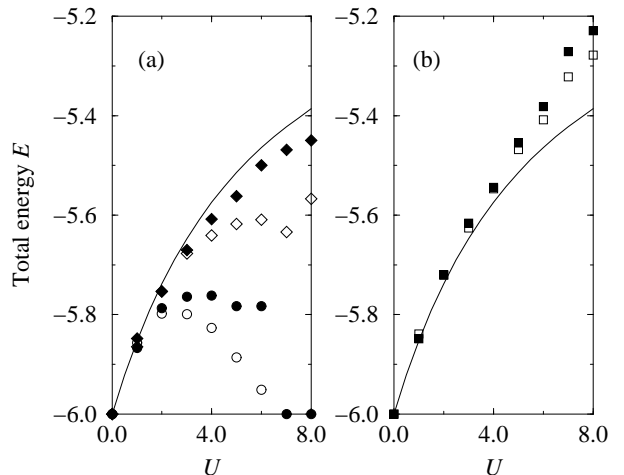


FIG. 5. Total energies calculated from (a) the  $GW$  and  $GWT$  approximations, indicated by circles and diamonds, respectively, and (b) the  $T_x$  scheme as a function of the interaction strength  $U$  for a low band filling of 17%. Open symbols refer to ordinary, non-self-consistent Green's functions, while filled symbols refer to self-consistent ones. The solid line shows the exact total energy for comparison.

corresponds to a low band filling of 17%, and  $N = 4$ , equivalent to an intermediate band filling of 33%. Results obtained from the  $GW$ , the  $GWT$ , and the  $T_x$  scheme are indicated by circles, diamonds, and squares, respectively. Open symbols refer to ordinary, non-self-consistent Green's functions, while filled symbols refer to self-consistent ones. The curves are not perfectly smooth due to unresolved convergence problems for individual values of  $U$ . As these do not obscure overall trends, however, we have decided to retain the corresponding energies for reasons of completeness. The solid line shows the exact total energy for comparison.

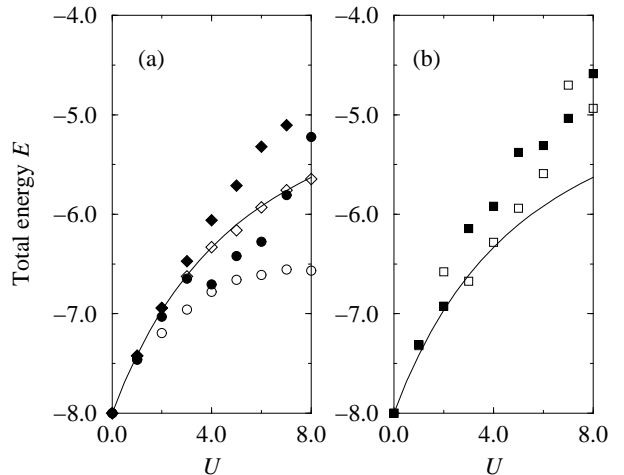


FIG. 6. Corresponding values for the same model with an intermediate band filling of 33%. Self-consistency systematically raises the total energy for all approximations.

As a first result we note that the quality of total-energy predictions correlates with that of spectral functions in the same parameter range, i.e., the Bethe–Goldstone approach works best for low particle numbers, while the two *GW* schemes perform optimally for intermediate band fillings, where screening effects dominate. Of the latter, the *GW* approximation is superior due to the prominence of exchange in the Hubbard model. The drop in the *GW* total energy after reaching a plateau is in part an artefact of the model specification: as the interaction is short-range, the true energy converges to a finite value in the limit  $U \rightarrow \infty$  as long as  $N \leq M$ , indicating a complete spatial separation of the electrons. The tendency of the *GW* approximation to underestimate the total energy eventually causes the downward trend. Such an unphysical behavior does not occur for the long-range Coulomb interaction, where the energy diverges as the correlation strength approaches infinity.

When comparing the total energies obtained from ordinary with those obtained from self-consistent Green's functions, we find that the latter are systematically raised. This is a general feature valid for all approximations at all band fillings that we investigated. It can be understood as follows: self-consistency modifies the Green's function in two ways, namely by rescaling and moving individual resonances relative to the chemical potential, and by an overall rigid shift caused by a redefinition of the chemical potential itself. The first effect may influence the total energy in either way, depending on the balance of opposite trends. For the homogeneous electron gas, for instance, the increase in band width, which moves quasiparticles to lower energies relative to the Fermi surface, competes with the upward transfer of spectral weight from low-lying plasmon satellites to the corresponding main peaks.<sup>19</sup> In contrast, the second contribution is always positive. It results from a relocation

of the chemical potential, which in an ordinary treatment is given by  $\mu = \mu^H + \langle \Sigma(\mu^H) \rangle$ , equivalent to that of the shifted Hartree Green's function in Dyson's equation. In a self-consistent approach the chemical potential instead becomes  $\mu = \mu^H + Z \langle \Sigma(\mu^H) \rangle$ , where  $Z$  is the quasiparticle renormalization factor. For the sake of the argument we ignore small deviations in the underlying Hartree potentials and the self-energy matrix elements, which are of course calculated from different Green's functions. It is then clear that in the self-consistent case the self-energy correction, which is always negative, is scaled down by  $Z$ , leading to a higher reference chemical potential. Unless compensated by other factors, this effect therefore always raises the total energy.

Although the argument makes the increase in total energy for the electron gas plausible, it does not explain the excellent numerical agreement with results from quantum Monte-Carlo simulations, which are presumed accurate. In the light of our calculations this appears rather fortuitous, however. While the increase in the *GW* total energy for our model system with two and four electrons indeed constitutes a quantitative improvement, in Fig. 7 we present results for a larger band filling of 67%, corresponding to  $N = 8$ , to demonstrate that this is not always so: as the ordinary *GW* approximation already predicts the true energies rather well in this case, self-consistency leads to a substantial overestimation.

## VI. CONCLUSIONS

In this paper we have presented self-consistent many-body calculations of the spectra and total energies for a model system. The self-consistency was not restricted and extends to the construction of the screened interaction in the random-phase approximation. By comparing the *GW* approximation with an extended *GWT* scheme that includes a nontrivial vertex function as well as the unrelated Bethe–Goldstone approach based on the *T*-matrix we were able to identify universal trends. We have demonstrated that the deterioration of spectral features due to self-consistency, previously observed in *GW* calculations, also occurs in more elaborate treatments and is not removed by vertex corrections. The most important effect is the broadening of satellite peaks, particularly at high energies, and their simultaneous shift towards the chemical potential. For all approximations the corresponding total energies are systematically raised. This trend, which we made plausible on the basis of physical arguments, is independent of the system parameters such as correlation strength and band filling. Our results therefore suggest that the recently reported improvement in the *GW* total energy for the electron gas due to self-consistency may be fortuitous.

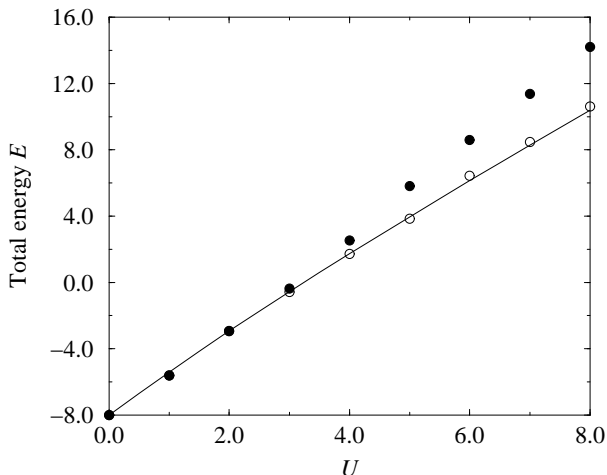


FIG. 7. Total energy in the *GW* approximation for a larger band filling of 67%. As the ordinary *GW* approximation already predicts the true energies rather well in this case, self-consistency leads to a substantial overestimation.

## ACKNOWLEDGMENTS

We are grateful to R. Haydock and C. M. M. Nex for helpful discussions. This work was supported by the Royal Society and the European Community program Human Capital and Mobility through contract No. CHRX-CT93-0337. A. Schindlmayr and T. J. Pollehn wish to thank the Studienstiftung des deutschen Volkes for financial support. A. Schindlmayr gratefully acknowledges further support from the Deutscher Akademischer Austauschdienst under its HSP III scheme, the Gottlieb Daimler- und Karl Benz-Stiftung, Pembroke College Cambridge, and the Engineering and Physical Sciences Research Council.

---

\* Electronic address: as10031@phy.cam.ac.uk

† Present address: The Boston Consulting Group, Sendlinger Straße 7, 80331 München, Germany.

<sup>1</sup> L. Hedin, Phys. Rev. **139**, A796 (1965).

<sup>2</sup> W.-D. Schöne and A. G. Eguiluz (unpublished).

<sup>3</sup> M. S. Hybertsen and S. G. Louie, Phys. Rev. Lett. **55**, 1418 (1985); Phys. Rev. B **32**, 7005 (1985); **34**, 5390 (1986).

<sup>4</sup> R. W. Godby, M. Schlüter, and L. J. Sham, Phys. Rev. Lett. **56**, 2415 (1986); Phys. Rev. B **35**, 4170 (1986); **37**, 10 159 (1988).

<sup>5</sup> W. von der Linden and P. Horsch, Phys. Rev. B **37**, 8351 (1988).

<sup>6</sup> J. E. Northrup, M. S. Hybertsen, and S. G. Louie, Phys. Rev. Lett. **59**, 819 (1987); Phys. Rev. B **39**, 8198 (1989); M. P. Surh, J. E. Northrup, and S. G. Louie, *ibid.* **38**, 5976 (1988).

<sup>7</sup> F. Aryasetiawan and U. von Barth, Physica Scripta **T45**, 270 (1992); F. Aryasetiawan, Phys. Rev. B **46**, 13 051 (1992).

<sup>8</sup> F. Aryasetiawan and O. Gunnarsson, Phys. Rev. Lett. **74**, 3221 (1995).

<sup>9</sup> A. Schindlmayr and R. W. Godby, Phys. Rev. Lett. **80**, 1702 (1998).

<sup>10</sup> T. J. Pollehn, A. Schindlmayr, and R. W. Godby, J. Phys.: Condens. Matter **10**, 1273 (1998).

<sup>11</sup> G. Baym and L. P. Kadanoff, Phys. Rev. **124**, 287 (1961).

<sup>12</sup> A. Schindlmayr, Phys. Rev. B **56**, 3528 (1997).

<sup>13</sup> M. Röhlffing, P. Krüger, and J. Pollmann, Phys. Rev. B **56**, R7065 (1997).

<sup>14</sup> U. von Barth and B. Holm, Phys. Rev. B **54**, 8411 (1996); **55**, 10 120(E) (1997).

<sup>15</sup> B. Holm and F. Aryasetiawan, Phys. Rev. B **56**, 12 825 (1997).

<sup>16</sup> E. L. Shirley, Phys. Rev. B **54**, 7758 (1996).

<sup>17</sup> B. Farid, Philos. Mag. B **76**, 145 (1997).

<sup>18</sup> H. J. de Groot, P. A. Bobbert, and W. van Haeringen, Phys. Rev. B **52**, 11 000 (1995).

<sup>19</sup> B. Holm and U. von Barth, Phys. Rev. B **57**, 2108 (1998).

<sup>20</sup> A. G. Eguiluz and W.-D. Schöne, Mol. Phys. **94**, 87 (1998).

<sup>21</sup> B. Schneider, H. S. Taylor, and R. Yaris, Phys. Rev. A **1**, 855 (1970).

<sup>22</sup> H. A. Bethe and J. Goldstone, Proc. R. Soc. London **A238**, 551 (1957).

<sup>23</sup> F. Aryasetiawan and O. Gunnarsson, Rep. Prog. Phys. **61**, 237 (1998).

<sup>24</sup> A. L. Fetter and J. D. Walecka, *Quantum Theory of Many-Particle Systems* (McGraw-Hill, San Francisco, 1971).

<sup>25</sup> B. N. Parlett, *The Symmetric Eigenvalue Problem* (Prentice Hall, Englewood Cliffs, 1980).

<sup>26</sup> R. Haydock, in *Solid State Physics*, edited by H. Ehrenreich, F. Seitz, and D. Turnbull (Academic, New York, 1980), Vol. 35, p. 215.

<sup>27</sup> H. N. Rojas, R. W. Godby, and R. J. Needs, Phys. Rev. Lett. **74**, 1827 (1995).

<sup>28</sup> E. L. Shirley and R. M. Martin, Phys. Rev. B **47**, 15 404 (1993).

<sup>29</sup> J. Kanamori, Prog. Theor. Phys. **30**, 275 (1963).

<sup>30</sup> M. Springer and F. Aryasetiawan, Phys. Rev. Lett. **80**, 2389 (1998).

<sup>31</sup> G. D. Mahan and B. E. Sernelius, Phys. Rev. Lett. **62**, 2718 (1989).

<sup>32</sup> C. Verdozzi, R. W. Godby, and S. Holloway, Phys. Rev. Lett. **74**, 2327 (1995).

<sup>33</sup> F. Bechstedt, K. Tenelsen, B. Adolph, and R. Del Sole, Phys. Rev. Lett. **78**, 1528 (1997).

<sup>34</sup> V. M. Galitskii and A. B. Migdal, Sov. Phys. JETP **7**, 96 (1958).

<sup>35</sup> A. Schindlmayr and R. W. Godby, Phys. Rev. B **51**, 10 427 (1995).